A non-catalytic function of PI3Kγ drives smooth muscle cell proliferation after arterial damage

Adrien Lupieri, Régis Blaise, Alessandra Ghigo, Natalia Smirnova, Marie-Kerguelen Sarthou, Nicole Malet, Isabelle Limon, Pierre Vincent, Emilio Hirsch, Stéphanie Gayral, et al.

© 2020. Published by The Company of Biologists Ltd | Journal of Cell Science (2020) 133, jcs245969. doi:10.1242/jcs.245969

SHORT REPORT

A non-catalytic function of PI3Kγ drives smooth muscle cell proliferation after arterial damage

Adrien Lupieri[1], Régis Blaise[2], Alessandra Ghigo[3], Natalia Smirnova[1], Marie-Kerguelen Sarthou[1], Nicole Malet[1], Isabelle Limon[2], Pierre Vincent[2], Emilio Hirsch[3], Stéphanie Gayral[1], Damien Ramel[1,*] and Muriel Laffargue[1,*]

ABSTRACT

Arterial remodeling in hypertension and intimal hyperplasia involves inflammation and disrupted flow, both of which contribute to smooth muscle cell dedifferentiation and proliferation. In this context, our previous results identified phosphoinositide 3-kinase γ (PI3Kγ) as an essential factor in inflammatory processes of the arterial wall. Here, we identify for the first time a kinase-independent role of nonhematopoietic PI3Kγ in the vascular wall during intimal hyperplasia using PI3Kγ-deleted mice and mice expressing a kinase-dead version of the enzyme. Moreover, we found that the absence of PI3Kγ in vascular smooth muscle cells (VSMCs) leads to modulation of cell proliferation, associated with an increase in intracellular cAMP levels. Real-time analysis of cAMP dynamics revealed that PI3Kγ modulates the degradation of cAMP in primary VSMCs independently of its kinase activity through regulation of the enzyme phosphodiesterase 4. Importantly, the use of an N-terminal competing peptide of PI3Kγ blocked primary VSMC proliferation. These data provide evidence for a kinase-independent role of PI3Kγ in arterial remodeling and reveal novel strategies targeting the docking function of PI3Kγ for the treatment of cardiovascular diseases.

KEY WORDS: PI3Kγ, Vascular smooth muscle cell, cAMP

INTRODUCTION

Vascular smooth muscle cells (VSMCs) are the unique component of the medial layer of normal arteries and are responsible for their contractile properties. In healthy conditions, VSMCs are mostly quiescent and differentiated, but can shift from the contractile to a so-called synthetic phenotype in which cells are able to migrate away from the medial layer of the artery to proliferate and accumulate in the intimal layer, leading to intimal hyperplasia (IH) in pathological conditions. Consequently, these processes induce intimal thickening and a reduction in blood flow, as observed during cardiovascular disease. Thus, understanding the mechanisms of VSMC proliferation is crucial for the development of new therapeutic strategies to prevent IH (Lacolley et al., 2018; Owens et al., 2004).

Among the signaling molecules involved in VSMC proliferation, the second messenger 3′,5′-cyclic adenosine monophosphate (cAMP) plays a major role. In VSMCs, elevated cAMP levels inhibit mitogen-stimulated proliferation both *in vitro* and *in vivo* (Bobin et al., 2016; Hewer et al., 2011; Indolfi et al., 2000; Smith et al., 2019). Consistently, cAMP has been found to play a positive role in reducing intimal thickening in several models of vascular injury. Moreover, cAMP signaling is affected in a large variety of vascular pathologies, including atherosclerosis and restenosis after angioplasty. cAMP signaling mainly depends on the localized production of cAMP by adenylyl cyclases (AC) and its degradation by nucleotide phosphodiesterases (PDEs) (Sassone-Corsi, 2012). In VSMCs, PDE3A, PDE4 and PDE1C have been implicated in the regulation of VSMC proliferation and IH (Begum et al., 2011; Bobin et al., 2016; Cai et al., 2015). Interestingly, it has been shown that cAMP production is linked to an increase in PDE4 activity and upregulated expression of the PDE4D isoform in both contractile and synthetic phenotypes (Tilley and Maurice, 2005). Consistently, numerous studies have been performed using PDE inhibitors in various arterial disease models (Bobin et al., 2016).

In this context, phosphoinositide 3-kinase γ (PI3Kγ; in which the catalytic subunit is known as p110γ or PIK3CG), a lipid kinase involved in the immune regulation of cardiovascular diseases, has been demonstrated to regulate cAMP levels in cardiomyocytes. Indeed, this kinase, which is known to generate 3-phosphoinositide lipid second messengers through its kinase activity, has also been demonstrated to act as an A-kinase anchoring protein (AKAP) to control cAMP levels in cardiac cells, leading to the modulation of cardiac contractility. Indeed, p110γ interacts with protein kinase A (PKA), which activates PDE3B to enhance cAMP degradation and phosphorylate p110γ to prevent phosphatidylinositol (3,4,5)-trisphosphate [PtdIns(3,4,5)P_3] production. Moreover, p110γ is also able to control cAMP levels through PDE4 in cardiomyocytes. Thus, PI3Kγ is a crossroad between the cAMP and PtdIns(3,4,5)P_3 signaling modules in cardiomyocytes (Ghigo et al., 2012; Patrucco et al., 2004; Perino et al., 2011; Voigt et al., 2005).

Here, using genetic approaches and a cutting-edge method for measuring cAMP, we highlight a link between PI3Kγ and cAMP signaling in VSMCs. We demonstrate that PI3Kγ regulates cAMP levels in primary VSMCs independently of its kinase activity and identify a PDE4 family enzyme as the predominant signaling partner of PI3Kγ in controlling VSMC proliferation involved in IH formation.

[1]Department of Vascular Biology of the Institute of Metabolic and Cardiovascular Diseases (I2MC), Université de Toulouse 3, Institut National de la Santé et de la Recherche Médicale (INSERM) UMR1048, Toulouse, France. [2]Sorbonne Université, Faculté des Sciences et Ingénierie, Institut de Biologie Paris-Seine (IBPS), UMR CNRS 8256 Adaptation Biologique et Vieillissement (B2A), 75005 Paris, France. [3]Department of Molecular Biotechnology and Health Sciences, Molecular Biotechnology Center, University of Torino, Via Nizza 52, 10126 Torino, Italy.

*Authors for correspondence (muriel.laffargue@inserm.fr; damien.ramel@inserm.fr)

P.V., 0000-0002-8479-1908; S.G., 0000-0001-6276-3917; D.R., 0000-0002-9089-1497; M.L., 0000-0003-1833-639X

Handling Editor: Kathleen Green
Received 10 March 2020; Accepted 14 May 2020

Journal of Cell Science (2020) 133, jcs245969. doi:10.1242/jcs.245969

RESULTS AND DISCUSSION

VSMC proliferation and intimal hyperplasia after injury is independent of the catalytic activity of PI3Kγ

Our previous results identified a role for PI3Kγ activity in the immune processes of IH development and arterial healing (Smirnova et al., 2014). This was demonstrated by using knock-in mice expressing an inactive PI3Kγ (PI3KγKD) subjected to arterial mechanical injury. To explore further the role of PI3Kγ in the vascular compartment, we generated bone marrow (BM) chimeras using PI3Kγ knockout (KO) and kinase-dead (KD) mice as recipients. This also allowed us to discriminate between the kinase-dependent and kinase-independent functions in the vascular compartment. We introduced BM from wild-type (WT) animals into PI3KγKO mice (WT>KO) or PI3KγKD mice (WT>KD) and vice versa (KO>WT and KD>WT). After engraftment, the injured femoral arteries were analyzed 28 days later. In BM WT>KO and BM KO>KO chimeras, the intima/media ratio was decreased by 40% compared with that in BM WT>WT chimeras (Fig. 1A,B), whereas no difference was observed for BM WT>KD chimeras. Moreover, BM KO>WT, BM KD>WT and KD>KD chimeras showed a decrease in the intima/media ratio, confirming the role of PI3Kγ activity in the immune compartment (Fig. 1A,B) (Smirnova et al., 2014). These results indicate that PI3Kγ, but not its catalytic activity, is required in the vascular compartment to induce a fibroproliferative response to injury. Histological analysis of the injured arteries by Masson's trichrome staining showed a decreased neointimal area in WT>KO and KO>WT BM chimeras compared with controls (Fig. 1A). These stainings indicate that this reduction in the neointimal area in WT>KO BM chimeras is mostly a result of the reduced expansion of the VSMC layer (Fig. 1A,B). Taken together these results demonstrate that VSMC proliferation postinjury is independent of the catalytic function of PI3Kγ but rather involves its docking function.

PI3Kγ docking function controls cAMP dynamics through PDE4D activity

Regarding the importance of cAMP in VSMC proliferation *in vitro* and *in vivo* (Bobin et al., 2016; Hewer et al., 2011; Indolfi et al., 2000), we hypothesized that PI3Kγ may also have a kinase-independent function in VSMCs via cAMP regulation. To test this hypothesis, the proliferation of primary VSMCs from mice of different genotypes (WT, PI3KγKO and PI3KγKD) was evaluated upon stimulation with platelet-derived growth factor (PDGF), a powerful mitogenic agent for VSMCs. An adenylate cyclase activator, forskolin, was added to the culture medium to increase cAMP levels and counterbalance VSMC proliferation induced by PDGF (Fig. 1C). Our results showed that 25µM forskolin decreased VSMC proliferation and that this effect was significantly potentiated in the absence of PI3Kγ (PI3KγKO VSMCs) but not in PI3KγKD VSMCs (Fig. 1D,E). These results suggest that PI3Kγ controls VSMC proliferation by regulating the intracellular concentration of cAMP independently of its enzymatic activity.

The involvement of PI3Kγ in controlling the intracellular concentration of cAMP in VSMC was confirmed by studying the dynamics of cAMP signals in primary VSMCs from WT, PI3KγKD and PI3KγKO mice using the FRET-based ^{T}Epac^{VV} biosensor (Klarenbeek et al., 2011). The relative changes in cAMP levels in response to 2.5 µM forskolin treatment were monitored over time by calculating the ratio of donor fluorescence (F480 nm) to acceptor fluorescence (F535 nm). The cAMP level was determined as a percentage of the maximum ratio change (R_{max}). R_{max} was determined at the end of the experiment by adding 200 µM 3-isobutyl-1-methylxanthine (IBMX), a pan-PDE inhibitor, in the presence of 2.5 µM forskolin. As shown in Fig. 2, cAMP production in response to 2.5 µM forskolin treatment was increased 2.2-fold in PI3KγKO VSMCs compared with WT primary VSMCs (24.1% versus 52.6% of the response to IBMX, P=0.03), whereas the response of PI3KγKD cells to forskolin was similar to that of WT cells (Fig. 2A,B; Fig. S1A). Basal cAMP levels were not altered in the steady state in any of the three genotypes (Fig. 2A,B). Moreover, the change in R_{max} was also identical in these VSMCs (Fig. 2A). Together, these results showed that the response of cAMP to forskolin was higher in PI3KγKO VSMCs than in WT and PI3KγKD cells, demonstrating a role for PI3Kγ in limiting the cAMP level.

The intracellular level of cAMP depends on cAMP production and degradation by AC and PDE, respectively. PI3Kγ has already been shown to bind PDE in cardiomyocytes (Perino et al., 2011). We focused on PDE3 and PDE4 because they have been implicated in IH (Begum et al., 2011; Inoue et al., 2000; Tilley and Maurice, 2005). We successively treated forskolin-stimulated VSMCs with cilostamide and rolipram, which target PDE3 and PDE4, respectively, and quantified cAMP levels according to the R_{max}. These experiments allowed us to evaluate the relative proportion of cAMP pools regulated by each PDE in the different genotypes. The results showed that cAMP levels were mostly regulated by PDE4 in WT and PI3KγKD cells (67% and 73%, respectively, relative to the response to IBMX). The effect of PDE3 on cAMP level regulation in these cells was limited to 25% and 17% of the response to IBMX, respectively (Fig. 3A–C). Accordingly, in PI3KγKO cells, the PDE isoform that degraded most cAMP was PDE3 (49% of the response to IBMX for PDE3 versus 43% for PDE4; Fig. 3C). To confirm the role of the PDE4 enzyme in cAMP regulation downstream of PI3Kγ, we performed immunoprecipitation and measured PDE4 activity. We focused on PDE4D, which is the main isoform expressed in VSMCs. Consistent with our cAMP measurements in living cells, PDE4D activity was significantly reduced in PI3KγKO cells compared with WT and PI3KγKD cells (Fig. 3D,E). Furthermore, knock down of PDE4D and PI3Kγ potentiated the effect of forskolin, as in PI3KγKO VSMCs, confirming the implication of these proteins in VSMC proliferation (Fig. S2A,B).

Interfering with PI3Kγ docking function using a permeant peptide impairs VSMC proliferation

PI3Kγ has been shown to regulate cAMP levels and signaling via its AKAP functions in cardiomyocytes (Perino et al., 2011). Interestingly, the interaction between PI3Kγ and the PKA/PDE complex has been mapped to amino acids 126 and 150 in the N-terminal region of p110γ (Perino et al., 2011). To investigate further the functional relationship between PI3Kγ, cAMP regulation by PKA/PDE and VSMC proliferation, we disrupted the PI3Kγ–PKA interaction by treating cells with a cell-penetrating competing peptide corresponding to the PKA binding region of p110γ and probed for their proliferation in response to PDGF and forskolin (Perino et al., 2011). A control peptide with two point mutations (K>A and R>A at positions 1 and 5, respectively) that does not interact with PKA was previously designed (Perino et al., 2011). We first determined the time course of peptide penetration into cells using a FITC-tagged version of the peptide. The peptide was detectable in cells after 5 h and still detectable 30 h after incubation (Fig. S3A,B). Therefore, we used this peptide to block the PI3Kγ–PKA interaction in the cell proliferation experiment, as shown in Fig. 1D. Incubation with the blocking peptide inhibited cell proliferation in WT and PI3KγKD cells (Fig. 4A,B), whereas no

Journal of Cell Science (2020) 133, jcs245969. doi:10.1242/jcs.245969

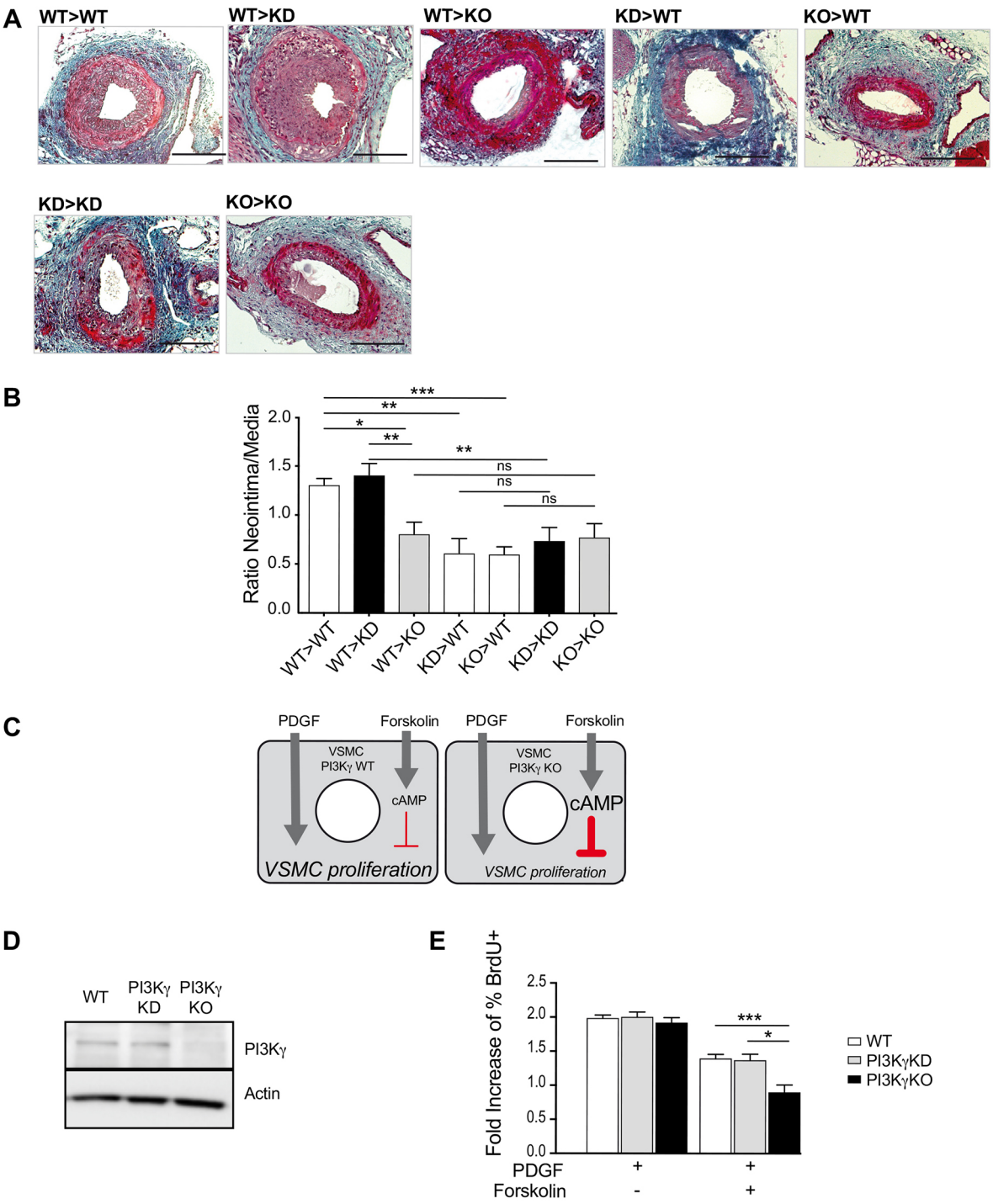

Fig. 1. PI3Kγ controls IH and VSMC proliferation. (A) Representative cross-sections of injured femoral arteries from the indicated hematopoietic chimeras stained with Masson's trichrome. Irradiated WT, PI3KγKD (KD) or PI3KγKO mouse recipients were transplanted with bone marrow (BM) from WT, KD or KO donors to obtain hematopoietic chimeras (BM WT>WT, BM WT>KD, BM WT>KO; BM KD>WT, BM KO>WT; BM KD>KD, BM KO>KO). (B) Quantitative analysis of the intima/media ratios of the indicated hematopoietic chimeras (n>6 mice for each group). (C) Representation of the experimental model used to investigate the role of PI3Kγ in the control of SMC proliferation. (D) Western blot of PI3Kγ expression in each genotype. (E) Proliferation rate of primary SMCs from WT, PI3KγKO and PI3KγKD mouse aortas incubated for 24 h with blocking medium (control) or treated with 25 ng/ml PDGF, with or without the addition of 25 µM forskolin, as measured by BrdU incorporation and expressed as the fold increase compared with control (5<n<12 cultures for each genotype). The data are presented as the mean±s.e.m. and were compared using one-way ANOVA; *P<0.05, **P<0.01, ***P<0.001; ns, not significant. Scale bars: 100 µM.

difference was observed in PI3KγKO cells (Fig. 4C). These data clearly demonstrated that PI3Kγ controlled VSMC proliferation via its AKAP function. Together, our results indicate that PI3Kγ acts as a catalyst of VSMC proliferation by decreasing cAMP levels, mainly through direct control of the PDE4 enzyme (Fig. 4D).

VSMC proliferation is a crucial aspect of the arterial response during various cardiovascular diseases, including IH. In our

Journal of Cell Science (2020) 133, jcs245969. doi:10.1242/jcs.245969

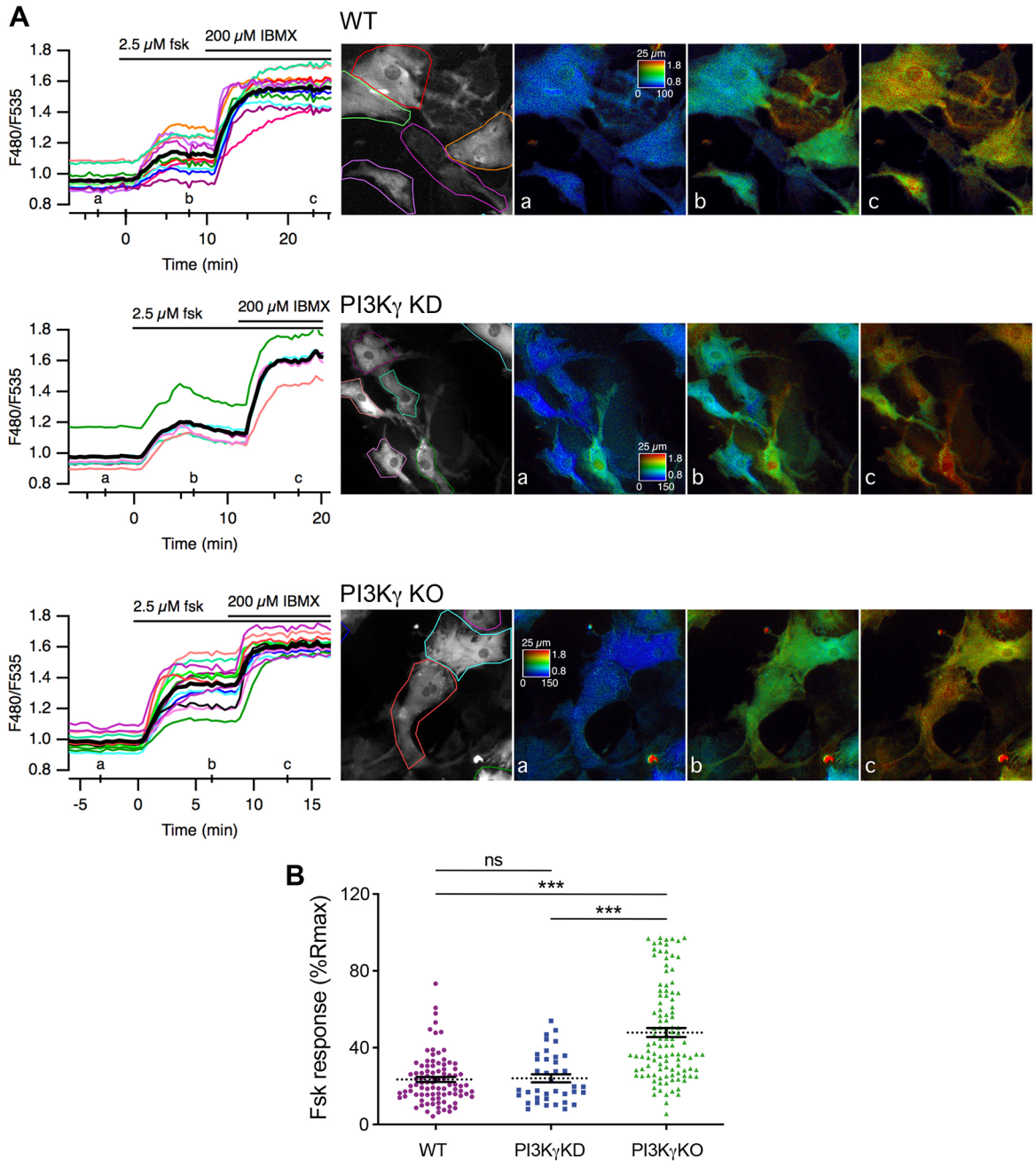

Fig. 2. PI3Kγ controls cAMP dynamics in VSMCs independently of its kinase activity. (A) Left: biosensor imaging of relative changes in the $[cAMP]_i$ in WT (top), PI3KγKD (middle) and PI3KγKO (bottom) primary VSMCs expressing the $^{T}Epac^{VV}$ biosensor. Each trace indicates the F480/F535 emission ratio over time in the regions of interest (ROI) defined for each cell. The black line represents the average of all traces. Right: microscopy fields in grayscale (left) showing the biosensor fluorescence at 535 nm. Pseudocolored images represent the F480/F535 ratio, which is indicative of the $[cAMP]_i$, before treatment (a), during 2.5 µM forskolin (fsk) stimulation (b) and during forskolin (2.5 µM) plus IBMX (200 µM) treatment (c). Calibration square indicates range intensity (counts/pixel/s) (horizontally) and the F480/F535 ratio (vertically). The F480/F535 ratio within the ROIs delimited by the colored contours was determined for individual cells. (B) Histograms representing the responses to forskolin. Results are expressed as a percentage of the maximum ratio change [$\%R_{max}$ (IBMX response)] determined by the final application of forskolin (2.5 µM) plus IBMX (200 µM) (n=92, 38 and 111 cells analyzed in WT, PI3KγKD and KO, respectively, from 5 different mice). The data are presented as the mean±s.e.m. and were compared using the Kruskal–Wallis test; ***P<0.01; ns, not significant.

study, we demonstrated that arterial PI3Kγ is an important factor in arterial remodeling in IH, independently of its kinase activity. We showed that PI3Kγ uses PDE4 enzymes to regulate cAMP levels to control VSMC proliferation. This finding is consistent with previous reports, which indicate that PDE4 is a crucial player in the synthetic phenotype (Tilley and Maurice, 2005).

A recent report indicated that PI3Kγ activity in VSMCs might represent a new therapeutic approach to treatment of IH (Yu et al., 2019). Consistent with our previous results, which demonstrated an important role for PI3Kγ activity in the T cell compartment after arterial injury (Lupieri et al., 2019; Smirnova et al., 2014), Yu and colleagues showed that PI3Kγ from bone marrow is involved in this pathology (Yu et al., 2019). In

Journal of Cell Science (2020) 133, jcs245969. doi:10.1242/jcs.245969

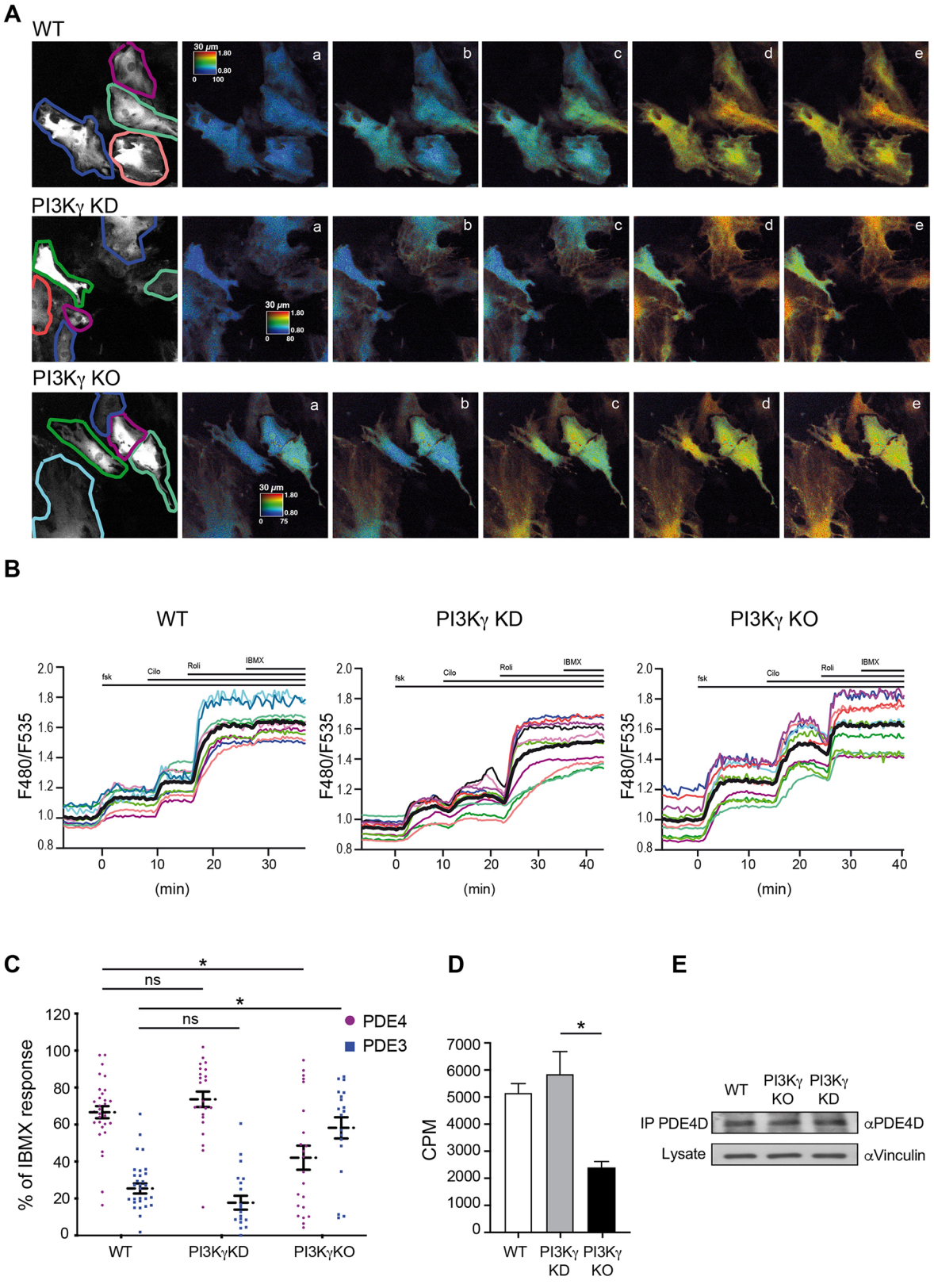

Fig. 3. See next page for legend.

addition, these authors claimed that PI3Kγ kinase activity controls VSMC proliferation in IH, whereas our data clearly demonstrated that PI3Kγ controls this effect independently of its kinase activity. Discriminating between the kinase-dependent and kinase-independent roles of PI3Kγ *in vivo* is only possible using a kinase-dead version of the enzyme (PI3KγKD). Our results clearly demonstrated that the absence of PI3Kγ activity in the nonhematopoietic compartment in PI3KγKD mice was not

Fig. 3. PI3Kγ controls cAMP levels in VSMCs via PDE4 activity. (A) Microscopy fields in grayscale (left) show the biosensor fluorescence at 535 nm. Pseudocolored images represent the F480/F535 ratio, which is indicative of the $[cAMP]_i$, before treatment (a), during 2.5 µM forskolin stimulation (b), during cilostamide treatment (1 µM) (c), during rolipram treatment (1 µM) (d) and during the application of forskolin (2.5 µM) plus IBMX (200 µM) (e). Calibration square indicates range intensity (counts/pixel/s) (horizontally) and the F480/F535 ratio (vertically). The F480/F535 ratio within the regions of interest (ROIs) delimited by the colored contours was determined for individual cells. (B) Biosensor imaging of relative changes in the $[cAMP]_i$ in WT (left), PI3KγKD (middle) and PI3KγKO (right) mouse primary VSMCs expressing the $^{T}Epac^{VV}$ biosensor. Each trace indicates the F480/F535 emission ratio over time in the ROI defined for each cell. The black line represents the average of all traces. (C) Histograms representing the mean values of forskolin responses. Results are expressed as a percentage of the maximum ratio change [$\%R_{max}$ (IBMX response)] determined by the final application of forskolin (2.5 µM) plus IBMX (200 µM). The data shown are mean±s.e.m. and were compared using the Kruskal–Wallis test (n>22 from 4 different mice). (D) Phosphodiesterase activity detected in PDE4D immunoprecipitates from primary VSMCs. The data shown are the mean± s.e.m. and were compared using one-way ANOVA followed by Bonferroni post hoc test (n=3). (E) Representative western blot of PDE4D immunoprecipitates. *P<0.05; ns, not significant.

sufficient to reduce IH, whereas deletion of the protein led to a large decrease in this process. Moreover, an N-terminal peptide containing residues 126–150 of PI3Kγ, which has previously been shown to disrupt the PKA–PI3Kγ interaction and decrease PDE3 activity in cardiomyocytes (Perino et al., 2011), abolished VSMC proliferation in response to PDGF and forskolin. Together, our results suggest that PI3Kγ activity inhibition is effective in preventing inflammation during IH due to its role in Th1 lymphocytes (Smirnova et al., 2014), whereas blocking its docking function would have a stronger effect on VSMC proliferation through modulation of cAMP levels.

In summary, we and others have demonstrated that PI3Kγ is at the crossroad between the cAMP and PtdIns(3,4,5)P_3 signaling modules (Perino et al., 2011), which are involved in several pathophysiological conditions, such as heart failure, blood–brain barrier integrity maintenance and arterial damage, leading to atherosclerosis or restenosis (Fougerat et al., 2008; Frister et al., 2014; Lupieri et al., 2019; Ndongson-Dongmo et al., 2015; Perino et al., 2011; Smirnova et al., 2014). Thus, PI3Kγ is an enzyme with dual roles, with two distinct possible therapeutic interventions to prevent arterial damages in cardiovascular disease.

MATERIALS AND METHODS

Animals

PI3Kγ-deficient (PI3KγKO) mice and PI3Kγ kinase-dead (PI3KγKD) mice, which express a catalytically inactive form of PI3Kγ, were on a C57BL/6J background and have been described previously (Fougerat et al., 2008; Hirsch et al., 2000; Patrucco et al., 2004). WT, PI3KγKD and PI3KγKO mice were maintained at the animal facility of Rangueil (UMS 006; Anexplo Platform) and kept under SPF conditions. All animal procedures were conducted in accordance with institutional guidelines on animal experimentation and were under a license from the French Ministry of Agriculture.

Femoral artery wire injury in mice

Male WT, PI3KγKD and PI3KγKO mice aged 8–10 weeks were investigated using an established model of femoral artery wire injury (Roque et al., 2000) for IH studies. In brief, general anesthesia was first achieved with 2% isoflurane. Then, the femoral artery was isolated and an incision made under a surgical microscope (Carl Zeiss, Germany). A 0.35 mm diameter angioplasty guide wire with a 0.25 mm tip (a gift from Abbott Vascular, Rungis, France) was advanced three times into the artery up to the level of the aortic bifurcation and then removed. After removal of the wire, the arteriotomy site was ligated. The mice were killed 28 days after the injury for histological and immunohistochemical analysis.

Tissue processing and morphometry

IH quantification was performed using the paraffin-embedment technique. After being euthanized, the mice were perfused with PBS followed by 4% paraformaldehyde. The vessels were harvested and fixed in 4% formalin, pH 8, for 24 h. Samples were put into paraffin and prepared as slides (sections 4 µm thick). To quantify the rate of IH, the sections were stained with Masson's Trichrome; then, the lumen, IEL (internal elastic lamina) and EEL (external elastic lamina) perimeters of each vessel were measured in four sections (at 0.5, 2.0, 3.5 and 5 mm from the ligation site) using LAS software (Leica). Arteries that underwent an occlusive thrombotic event were excluded from the quantification. Areas (A µm^2) were calculated from the perimeter measurements assuming circular geometry. The area defined by the EEL *in vivo* was calculated using the formula A_{EEL}=EEL circumference^2/4π. The area defined by the IEL was calculated using the formula A_{IEL}=IEL circumference^2/4π. The lumen area was calculated using the formula A_{LUM}=Lumen circumference^2/4π. The neointimal area was calculated using the formula $A_{NEO}=A_{IEL}-A_{LUM}$. The medial area was calculated using the formula $A_{MED}=A_{EEL}-A_{IEL}$. The intima/media ratio was calculated as A_{NEO}/A_{MED}.

BM transplantation

BM was obtained from 8-week-old WT, PI3KγKD and PI3KγKO mice. BM cells were flushed from the femurs and tibias, washed, filtered, counted and resuspended in sterile PBS. Then, 10^7 unfractionated cells were retro-orbitally injected into each irradiated (9 Gy) WT, PI3KγKD or PI3KγKO mouse. Four weeks later, femoral artery injury was performed and the mice euthanized 28 days after the surgery. Successful BM engraftment was confirmed by measuring WT DNA by polymerase chain reaction (PCR) from BM cells of different chimeric mice using a semi-quantitative analysis as previously described (Gayral et al., 2014).

Isolation of VSMCs from mouse aortas and culture

Mouse VSMCs were isolated from WT mice according to a previously described protocol, with modifications (Ray et al., 2001). In brief, the aorta from WT, PI3KγKD or PI3KγKO mice were dissected from the origin to the iliac bifurcation, flushed with PBS and removed. The adventitia was removed from the aortas, and the smooth tubes were cut into 1-2 mm pieces and digested in 0.3% collagenase solution. Collagenase digestion was stopped by the addition of Dulbecco's modified Eagle medium (DMEM; D0822, Sigma Aldrich, St Louis, MO) and 10% FBS. Then, the pieces of aorta were washed twice and seeded in culture dishes. Primary confluent cultures were trypsinized (0.1% trypsin; Thermo Fisher Scientific) at 37°C and the cells cultured until the fourth passage in DMEM with 10% FBS at 37°C and 5% CO_2.

Measure of mouse VSMC proliferation

Primary mouse VSMCs were subcultured in 48-well cell culture plates in complete medium. The cells were incubated with or without PDGF (520-BB-050, R&D Systems) and forskolin (F3917, Sigma Aldrich) for 24 h. For blocking peptide experiments, the cells were incubated for 24 h with 25 µM control peptide (RQIKIWFQNRRMKWKKGAATHASPGQIHLVQRHP-PSEESQAF) or blocking peptide (RQIKIWFQNRRMKWKKGKATHR-SPGQIHLVQRHPPSEESQAF). BrdU (00-0103, Invitrogen) incorporation assays were performed by classical immunofluorescence using an anti-BrdU antibody (11-5071, eBioscience) and DAPI. The proliferation rate was measured as the ratio of BrdU-positive nuclei to total nuclei and expressed as the fold increase. For A7r5 primary VSMCs, proliferation rate was measured with the cell proliferation kit II (XTT; Roche) according to the manufacturer instructions and the rate expressed as the fold increase.

Cell culture and transfections

A7r5 (ATCC CRL1444) VSMCs were cultured at 37°C and 5% CO_2 in DMEM supplemented with 10% FBS. siRNA transfections were performed using Lipofectamine RNAi Max (Invitrogen, Life Technologies) according to the manufacturer's instructions; siRNAs were used at a final

Journal of Cell Science (2020) 133, jcs245969. doi:10.1242/jcs.245969

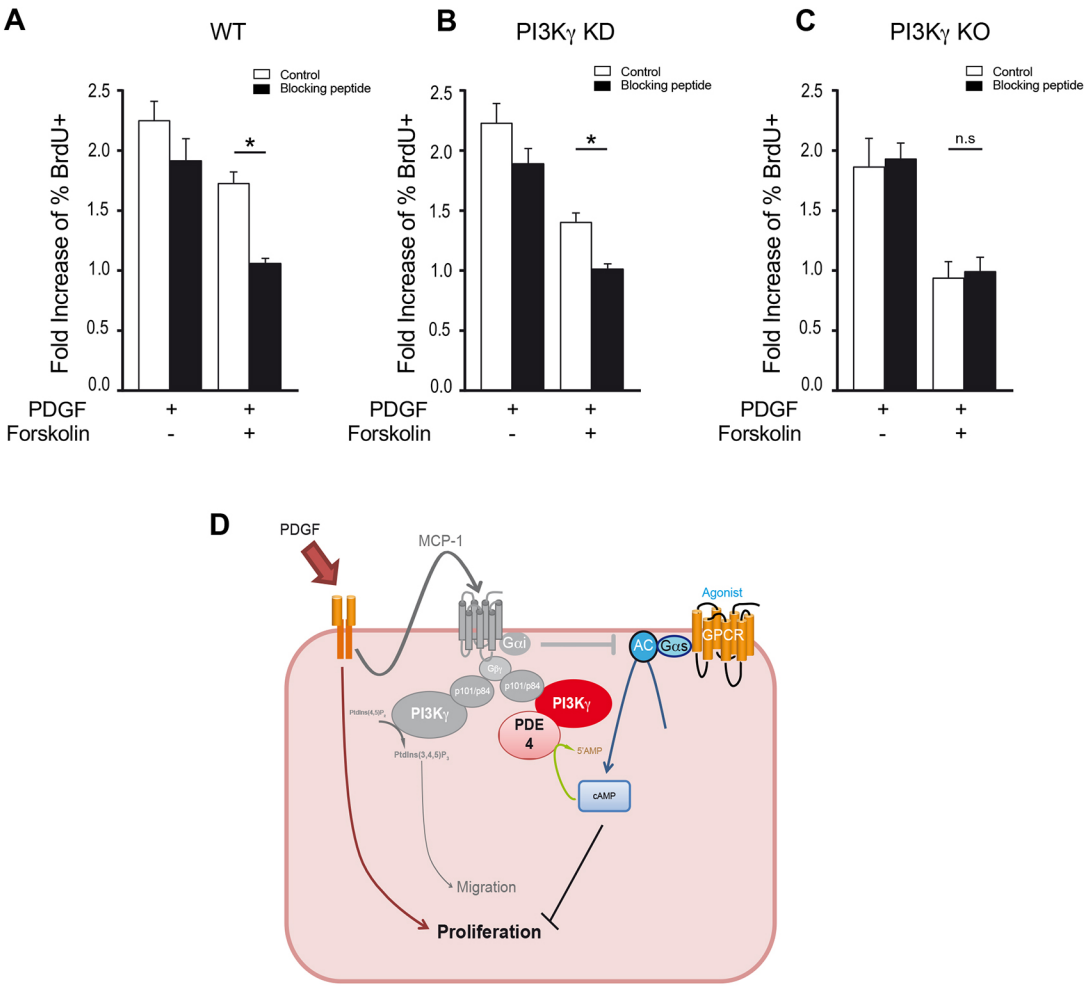

Fig. 4. A permeant N-terminal peptide of PI3Kγ impacts VSMC proliferation. (A–C) Proliferation rate of primary VSMCs from WT (A), PI3KγKD (B) and PI3KγKO (C) mouse aortas incubated for 24 h in the presence of 25 µM control (white bar) or blocking peptide (black bar) with blocking medium or treated with 25 ng/ml PDGF with or without the addition of 25 µM forskolin, as measured by BrdU incorporation and expressed as the fold increase compared with cells incubated with blocking medium alone. BrdU was added during the last 18 h (*n*=8 cultures for each genotype). Data are presented as the mean±s.e.m. and were compared using one-way ANOVA. (D) Model of the role of PI3Kγ in VSMC proliferation. Our previous results (in gray) demonstrated that the autocrine secretion of MCP1 recruits and activates PI3Kγ through GPCR signaling to control cell migration after PDGF stimulation (Fougerat et al., 2012). This PI3Kγ recruitment can also concentrate phosphodiesterases (PDEs) that counterbalance cAMP production by adenylate cyclase (AC) induced by other signals. Through these mechanisms, PI3Kγ acts as an amplifier of VSMC synthetic transition. **P*<0.05; n.s, not significant.

concentration of 20 nM. All siRNAs were purchased from Qiagen. RNAi sequences were as follows: rat PI3Kγ, 5′-ACACUAUCAGCAGAGGUU-CTT-3′ and rat PDE4D, 5′-ACUUUGAUUACGUAUCUUATT-3′.

Real time quantitative PCR

RNA was extracted using TRIzol reagent (Life technologies). *PI3Kγ* and *PDE4D* mRNA expression was analyzed from cDNA by real-time quantitative PCR using SyBR Green Light-Cycler480 technology (Roche). Relative mRNA expression was performed using the classic ΔΔCt method with the *Rpl13* gene as a reference and was expressed as fold increase over control. Primer sequences were as follows: rat PI3Kγ forward, 5′-GCAGAAGAGTCTCGAGCAGTG-3′ and reverse, 5′-CGGAGGTTG-TCCTCTCTCAG-3′. Rat PDE4D forward, 5′-ACCCATGTGCAACCAA-CCATCC-3′ and reverse, 5′-AGTTTCTGGTAGGCCTCCTCTGTG-3′.

Western blot analysis

Proteins from primary VSMCs were dissolved in Laemmli buffer, boiled, separated by SDS-polyacrylamide gel electrophoresis and transferred onto a nitrocellulose membrane. Immunodetection was achieved using the indicated primary antibodies overnight at 4°C. PI3Kγ monoclonal antibody was previously described (Hirsch et al., 2000) and rabbit anti-PDE4D antibody was obtained from Abcam (ab171750). Membranes were then incubated with HRP-conjugated secondary antibody (anti-mouse or anti-rabbit, 1:1000) for 1 h at room temperature. Immunoreactive proteins were detected with ECL reagents according to the manufacturer's instructions.

Measurement of cAMP dynamics

Primary VSMCs were seeded on coverslips and infected with the ^{T}Epac^{VV}-encoding type-5 adenovirus (~100 particles per VSMC) as described elsewhere (Vallin et al., 2018). Coverslips were placed in a microscope chamber continually perfused (2 ml/min) with BBS buffer (125 mM NaCl, 2 mM $CaCl_2$, 1 mM $MgCl_2$, 1.25 mM NaH_2PO_4, 26 mM $NaHCO_3$ and 25 mM glucose) saturated with 95% O_2 and 5% CO_2. Ratiometric analyses were performed as follows: fluorophores were excited with an LED source at 435 nm and the fluorescence emission monitored with a dichroic mirror (T450LPXR) and alternating emission filters for the donor (HQ480/40) and acceptor (D535/40). Pairs of images were recorded with an Orca-ER CCD camera (Hamamatsu Photonics, Japan) at 20 s intervals. Changes in the intracellular cAMP concentration $[cAMP]_i$, were expressed as changes in

the ratio of donor fluorescence (F480) to acceptor fluorescence (F535). The ratios were multiplied by the same constant for all experiments such that the baseline ratio was 1 under basal conditions. The maximum ratio change (R_{max}) was obtained after stimulating cells with 2.5 µM forskolin and 200 µM IBMX (I5879, Sigma Aldrich). Filters and mirrors were obtained from AHF Analysentechnik (Tübingen, Germany).

Measurement of cAMP intracellular levels

The amount of cAMP in primary VSMCs was measured by HTRF (homogeneous time-resolved FRET) kit cAMP-femto (62AM7PEB, Cisbio) in accordance with the manufacturer's instructions. Briefly, the cells in suspension were incubated with or without forskolin for 30 min. Cells were then lysed in the presence of cAMP conjugated to fluorochrome d2 (665 nm emission) and incubated with an anti-cAMP antibody conjugated to fluorochrome cryptate-Tb (emission 620 nm) for 1 h. We used microplate reader (Tecan) to measure the FRET signal (ratio 665 nm/620 nm) after excitation of cryptate-Tb at 320 nm.

Measurement of PDE activity

Cells were scraped in 120 mmol/l NaCl, 50 mmol/l Tris-HCl (pH 8.0) and 1% Triton X-100 supplemented with protease and phosphatase inhibitors and centrifuged at 16,000 ***g*** for 10 min at 4°C. The supernatants were subjected to immunoprecipitation and then assayed for PDE activity or used for western blotting. For immunoprecipitation assays, 200 µg of precleared extracts were incubated for 2 h at 4°C with 20 µl of a 1:1 slurry of protein A- and G-Sepharose (Amersham Biosciences, Buckinghamshire, UK) and 1 µg of antibody. The immunocomplexes were then extensively washed with lysis buffer and subjected to PDE activity assays. PDE activity in the immunoprecipitates was measured according to the two-step method of Thompson and Appleman with minor modifications (Thompson and Appleman, 1971). In brief, the immunoprecipitates were assayed in a total volume of 200 µl of reaction mixture containing 40 mmol/l Tris-HCl (pH 8.0), 1 mmol/l $MgCl_2$, 1.4 mmol/l 2-mercaptoethanol, 1 µmol/l cAMP (Sigma-Aldrich) and 0.1 µCi [^{3}H]cAMP (Amersham Bioscience, Buckinghamshire, UK) for 45 min at 33°C. To stop the reaction, the samples were boiled at 95°C for 3 min. The PDE reaction product 5′-AMP was then hydrolyzed by incubating the assay mixture with 50 µg of *Crotalus atrox* snake venom for 15 min at 37°C (Sigma-Aldrich). The resulting adenosine was separated by anion exchange chromatography using 400 µl of a 30% (w/v) suspension of Dowex AG1-X8 resin (Bio-Rad, Segrate, Milano, Italy). The amount of radiolabeled adenosine in the supernatant was quantified by scintillation counting (Ultima Gold scintillation liquid, Perkin Elmer, Waltham, MA).

Statistical analysis

The statistical significance of differences between multiple groups were determined using one-way analysis of variance (ANOVA) followed by Bonferroni's post hoc test. cAMP measurements using biosensor were analyzed using the Kruskal–Wallis test. Values of $P<0.05$ were considered statistically significant. All statistical analyses were performed using the GraphPad Prism software.

Acknowledgements

We thank Genotoul Anexplo US006/INSERM/UPS and Toulouse, the TRI-Genotoul Platform of Toulouse (I2MC/UMR1048) and the Non-Invasive Exploration Service.

Competing interests

The authors declare no competing or financial interests.

Author contributions

Conceptualization: A.L., I.L., P.V., S.G., D.R., M.L.; Methodology: A.L., R.B., P.V., M.L.; Validation: I.L., P.V., E.H., S.G., D.R., M.L.; Formal analysis: A.L., R.B., I.L., P.V., D.R., M.L.; Investigation: A.L., R.B., A.G., N.S., M.-K.S., N.M., S.G., D.R.; Writing - original draft: D.R.; Writing - review & editing: R.B., P.V., S.G., D.R., M.L.; Visualization: M.L.; Supervision: D.R., M.L.; Project administration: M.L.; Funding acquisition: M.L.

Funding

This work was supported by Institut National de la Santé et de la Recherche Médicale (INSERM), Université de Toulouse, Fondation pour la Recherche Médicale (FRM DPC20171138962), Fondation de France (Grant 201600066679) and Agence Nationale de la Recherche (ANR)-JCJC (ANR-12-JSV1-0006-01) to M.L.

Supplementary information

Supplementary information available online at
https://jcs.biologists.org/lookup/doi/10.1242/jcs.245969.supplemental

Peer review history

The peer review history is available online at
https://jcs.biologists.org/lookup/doi/10.1242/jcs.245969.reviewer-comments.pdf

References

Begum, N., Hockman, S. and Manganiello, V. C. (2011). Phosphodiesterase 3A (PDE3A) deletion suppresses proliferation of cultured murine vascular smooth muscle cells (VSMCs) via inhibition of mitogen-activated protein kinase (MAPK) signaling and alterations in critical cell cycle regulatory proteins. *J. Biol. Chem.* **286**, 26238-26249. doi:10.1074/jbc.M110.214155

Bobin, P., Belacel-Ouari, M., Bedioune, I., Zhang, L., Leroy, J., Leblais, V., Fischmeister, R. and Vandecasteele, G. (2016). Cyclic nucleotide phosphodiesterases in heart and vessels: a therapeutic perspective. *Arch. Cardiovasc. Dis.* **109**, 431-443. doi:10.1016/j.acvd.2016.02.004

Cai, Y., Nagel, D. J., Zhou, Q., Cygnar, K. D., Zhao, H., Li, F., Pi, X., Knight, P. A. and Yan, C. (2015). Role of cAMP-phosphodiesterase 1C signaling in regulating growth factor receptor stability, vascular smooth muscle cell growth, migration, and neointimal hyperplasia. *Circ. Res.* **116**, 1120-1132. doi:10.1161/CIRCRESAHA.116.304408

Fougerat, A., Gayral, S., Gourdy, P., Schambourg, A., Ruckle, T., Schwarz, M. K., Rommel, C., Hirsch, E., Arnal, J. F., Salles, J. P. et al. (2008). Genetic and pharmacological targeting of phosphoinositide 3-kinase-gamma reduces atherosclerosis and favors plaque stability by modulating inflammatory processes. *Circulation* **117**, 1310-1317. doi:10.1161/CIRCULATIONAHA.107.720466

Fougerat, A., Smirnova, N. F., Gayral, S., Malet, N., Hirsch, E., Wymann, M. P., Perret, B., Martinez, L. O., Douillon, M. and Laffargue, M. (2012). Key role of PI3Kγ in monocyte chemotactic protein-1-mediated amplification of PDGF-induced aortic smooth muscle cell migration. *Br. J. Pharmacol.* **166**, 1643-1653. doi:10.1111/j.1476-5381.2012.01866.x

Frister, A., Schmidt, C., Schneble, N., Brodhun, M., Gonnert, F. A., Bauer, M., Hirsch, E., Muller, J. P., Wetzker, R. and Bauer, R. (2014). Phosphoinositide 3-kinase γ affects LPS-induced disturbance of blood-brain barrier via lipid kinase-independent control of cAMP in microglial cells. *Neuromolecular Med.* **16**, 704-713. doi:10.1007/s12017-014-8320-z

Gayral, S., Garnotel, R., Castaing-Berthou, A., Blaise, S., Fougerat, A., Berge, E., Montheil, A., Malet, N., Wymann, M. P., Maurice, P. et al. (2014). Elastin-derived peptides potentiate atherosclerosis through the immune Neu1-PI3Kγ pathway. *Cardiovasc. Res.* **102**, 118-127. doi:10.1093/cvr/cvt336

Ghigo, A., Perino, A., Mehel, H., Zahradnikova, A., Jr, Morello, F., Leroy, J., Nikolaev, V. O., Damilano, F., Cimino, J., De Luca, E. et al. (2012). Phosphoinositide 3-kinase gamma protects against catecholamine-induced ventricular arrhythmia through protein kinase A-mediated regulation of distinct phosphodiesterases. *Circulation* **126**, 2073-2083. doi:10.1161/CIRCULATIONAHA.112.114074

Hewer, R. C., Sala-Newby, G. B., Wu, Y.-J., Newby, A. C. and Bond, M. (2011). PKA and Epac synergistically inhibit smooth muscle cell proliferation. *J. Mol. Cell. Cardiol.* **50**, 87-98. doi:10.1016/j.yjmcc.2010.10.010

Hirsch, E., Katanaev, V. L., Garlanda, C., Azzolino, O., Pirola, L., Silengo, L., Sozzani, S., Mantovani, A., Altruda, F. and Wymann, M. P. (2000). Central role for G protein-coupled phosphoinositide 3-kinase gamma in inflammation. *Science* **287**, 1049-1053. doi:10.1126/science.287.5455.1049

Indolfi, C., Di Lorenzo, E., Rapacciuolo, A., Stingone, A. M., Stabile, E., Leccia, A., Torella, D., Caputo, R., Ciardiello, F., Tortora, G. et al. (2000). 8-chloro-cAMP inhibits smooth muscle cell proliferation in vitro and neointima formation induced by balloon injury in vivo. *J. Am. Coll. Cardiol.* **36**, 288-293. doi:10.1016/S0735-1097(00)00679-3

Inoue, Y., Toga, K., Sudo, T., Tachibana, K., Tochizawa, S., Kimura, Y., Yoshida, Y. and Hidaka, H. (2000). Suppression of arterial intimal hyperplasia by cilostamide, a cyclic nucleotide phosphodiesterase 3 inhibitor, in a rat balloon double-injury model. *Br. J. Pharmacol.* **130**, 231-241. doi:10.1038/sj.bjp.0703287

Klarenbeek, J. B., Goedhart, J., Hink, M. A., Gadella, T. W. J. and Jalink, K. (2011). A mTurquoise-based cAMP sensor for both FLIM and ratiometric read-out has improved dynamic range. *PLoS ONE* **6**, e19170. doi:10.1371/journal.pone.0019170

Lacolley, P., Regnault, V. and Avolio, A. P. (2018). Smooth muscle cell and arterial aging: basic and clinical aspects. *Cardiovasc. Res.* **114**, 513-528. doi:10.1093/cvr/cvy009

Lupieri, A., Smirnova, N. F., Solinhac, R., Malet, N., Benamar, M., Saoudi, A., Santos-Zas, I., Zeboudj, L., Ait-Oufella, H., Hirsch, E. et al. (2019). Smooth muscle cells-derived CXCL10 prevents endothelial healing through PI3Kgamma-dependent T cells response. *Cardiovasc. Res.* **116**, 438-449. doi:10.1093/cvr/cvz122

Ndongson-Dongmo, B., Heller, R., Hoyer, D., Brodhun, M., Bauer, M., Winning, J., Hirsch, E., Wetzker, R., Schlattmann, P. and Bauer, R. (2015). Phosphoinositide 3-kinase gamma controls inflammation-induced myocardial depression via sequential cAMP and iNOS signalling. *Cardiovasc. Res.* **108**, 243-253. doi:10.1093/cvr/cvv217

Owens, G. K., Kumar, M. S. and Wamhoff, B. R. (2004). Molecular regulation of vascular smooth muscle cell differentiation in development and disease. *Physiol. Rev.* **84**, 767-801. doi:10.1152/physrev.00041.2003

Patrucco, E., Notte, A., Barberis, L., Selvetella, G., Maffei, A., Brancaccio, M., Marengo, S., Russo, G., Azzolino, O., Rybalkin, S. D. et al. (2004). PI3Kγ modulates the cardiac response to chronic pressure overload by distinct kinase-dependent and -independent effects. *Cell* **118**, 375-387. doi:10.1016/j.cell.2004.07.017

Perino, A., Ghigo, A., Ferrero, E., Morello, F., Santulli, G., Baillie, G. S., Damilano, F., Dunlop, A. J., Pawson, C., Walser, R. et al. (2011). Integrating cardiac PIP3 and cAMP signaling through a PKA anchoring function of p110γ. *Mol. Cell* **42**, 84-95. doi:10.1016/j.molcel.2011.01.030

Ray, J. L., Leach, R., Herbert, J. M. and Benson, M. (2001). Isolation of vascular smooth muscle cells from a single murine aorta. *Methods Cell Sci.* **23**, 185-188. doi:10.1023/A:1016357510143

Roque, M., Fallon, J. T., Badimon, J. J., Zhang, W. X., Taubman, M. B. and Reis, E. D. (2000). Mouse model of femoral artery denudation injury associated with the rapid accumulation of adhesion molecules on the luminal surface and recruitment of neutrophils. *Arterioscler. Thromb. Vasc. Biol.* **20**, 335-342. doi:10.1161/01.atv.20.2.335

Sassone-Corsi, P. (2012). The cyclic AMP pathway. *Cold Spring Harb. Perspect. Biol.* **4**, a011148. doi:10.1101/cshperspect.a011148

Smirnova, N. F., Gayral, S., Pedros, C., Loirand, G., Vaillant, N., Malet, N., Kassem, S., Calise, D., Goudouneche, D., Wymann, M. P. et al. (2014). Targeting PI3Kγ activity decreases vascular trauma-induced intimal hyperplasia through modulation of the Th1 response. *J. Exp. Med.* **211**, 1779-1792. doi:10.1084/jem.20131276

Smith, S. A., Newby, A. C. and Bond, M. (2019). Ending restenosis: inhibition of vascular smooth muscle cell proliferation by cAMP. *Cells* **8**, E1447. doi:10.3390/cells8111447

Thompson, W. J. and Appleman, M. M. (1971). Characterization of cyclic nucleotide phosphodiesterases of rat tissues. *J. Biol. Chem.* **246**, 3145-3150.

Tilley, D. G. and Maurice, D. H. (2005). Vascular smooth muscle cell phenotype-dependent phosphodiesterase 4D short form expression: role of differential histone acetylation on cAMP-regulated function. *Mol. Pharmacol.* **68**, 596-605. doi:10.1124/mol.105.014126

Vallin, B., Legueux-Cajgfinger, Y., Clément, N., Glorian, M., Duca, L., Vincent, P., Limon, I. and Blaise, R. (2018). Novel short isoforms of adenylyl cyclase as negative regulators of cAMP production. *Biochim. Biophys. Acta. Mol. Cell Res.* **1865**, 1326-1340. doi:10.1016/j.bbamcr.2018.06.012

Voigt, P., Brock, C., Nurnberg, B. and Schaefer, M. (2005). Assigning functional domains within the p101 regulatory subunit of phosphoinositide 3-kinase γ. *J. Biol. Chem.* **280**, 5121-5127. doi:10.1074/jbc.M413104200

Yu, Q., Li, W., Jin, R., Yu, S., Xie, D., Zheng, X., Zhong, W., Cheng, X., Hu, S., Li, M. et al. (2019). PI3Kgamma (phosphoinositide 3-kinase gamma) regulates vascular smooth muscle cell phenotypic modulation and neointimal formation through CREB (cyclic AMP-response element binding protein)/YAP (yes-associated protein) signaling. *Arterioscler. Thromb. Vasc. Biol.* **39**, e91-e105. doi:10.1161/ATVBAHA.118.312212